Available online at www.sciencedirect.com
ScienceDirect
Journal of Environmental Sciences 2012, 24(2) 261–268
JOURNAL OF ENVIRONMENTAL SCIENCES
ISSN 1001-0742
CN 11-2629/X
www.jesc.ac.cn

Acid Blue 25 adsorption on base treated *Shorea dasyphylla* sawdust: Kinetic, isotherm, thermodynamic and spectroscopic analysis

Megat Ahmad Kamal Megat Hanafiah[1,*], Wan Saime Wan Ngah[2], Shahira Hilwani Zolkafly[2], Lee Ching Teong[2], Zafri Azran Abdul Majid[3]

1. Department of Chemistry, Faculty of Applied Sciences, Universiti Teknologi MARA, 26400, Jengka, Pahang, Malaysia. E-mail: makmh73@yahoo.com.my
2. School of Chemical Sciences, Universiti Sains Malaysia, 11800, Minden, Penang, Malaysia
3. Kulliyyah of Allied Health Sciences, International Islamic University Malaysia, 25200, Kuantan, Pahang, Malaysia

Received 22 January 2011; revised 25 May 2011; accepted 30 May 2011

Abstract

The potential of base treated *Shorea dasyphylla* (BTSD) sawdust for Acid Blue 25 (AB 25) adsorption was investigated in a batch adsorption process. Various physiochemical parameters such as pH, stirring rate, dosage, concentration, contact time and temperature were studied. The adsorbent was characterized with Fourier transform infrared spectrophotometer, scanning electron microscope and Brunauer, Emmett and Teller analysis. The optimum conditions for AB 25 adsorption were pH 2, stirring rate 500 r/min, adsorbent dosage 0.10 g and contact time 60 min. The pseudo second-order model showed the best conformity to the kinetic data. The equilibrium adsorption of AB 25 was described by Freundlich and Langmuir, with the latter found to agree well with the isotherm model. The maximum monolayer adsorption capacity of BTSD was 24.39 mg/g at 300 K, estimated from the Langmuir model. Thermodynamic parameters such as Gibbs free energy, enthalpy and entropy were determined. It was found that AB 25 adsorption was spontaneous and exothermic.

Key words: Acid Blue 25; adsorption; *Shorea dasyphylla* sawdust; spectroscopy; thermodynamic
DOI: 10.1016/S1001-0742(11)60764-X

Introduction

The release of synthetic dyes into the ecosystem is a major source of aesthetic problem and can be harmful to aquatic life. Textile, paper mills and leather are among the major industries that release hazardous dyes into the environment (Mui et al., 2010a). According to Garg et al. (2004), dyes impede light penetration, retard photosynthetic activity, inhibit the growth of biota, and have a tendency to chelate metal ions. Removing synthetic dyes from the industrial effluents is a great challenge since most dyes are stable to light and heat, high in organic content, have complex aromatic structures and not biodegradable. A number of organic (Azlan et al., 2009; Saha, 2010) and inorganic adsorbents (Atar and Olgun, 2007; Ferrero, 2010), composites (Anirudhan and Suchithra, 2009; Liu et al., 2010) and microorganisms (Ali, 2010; Çolaklak et al., 2009; Wu et al., 2009) have been used for dyes removal. Activated carbon is the most commonly used adsorbent nowadays due to its large surface area (Tsang et al., 2007), but its high cost limits its application. As an alternative way to reduce costs, many agricultural wastes and byproducts of wood and forest industries of cellulose origin have been successfully utilized, including sawdust (Özacar and Şengil, 2005; Shi et al., 2007), palm kernel seed (Oladoja and Akinlabi, 2009), hazelnut shells (Ferrero, 2007) and fibers (Ghali et al., 2010). Dried activated sludge has also been used to remove reactive and basic dyes (Batzias and Sidiras, 2007).

This project attempts to remove Acid Blue 25 (AB 25) from aqueous solutions by base treated *Shorea dasyphylla* (BTSD) sawdust as an adsorbent. In Malaysia, *Shorea dasyphylla* (SD) sawdust is in abundance and is generated from furniture industries. The sawdust was treated with a strong alkaline solution (NaOH) to remove pectin, lignin and hemicelluloses (Ghali et al., 2010) and liberate new adsorption sites on the sawdust surface. This type of treatment was effective for removing toxic heavy metal ions (Wan Ngah and Hanafiah, 2008a). The reactions that took place can be represented as follows:

carboxylic acid:

$$-\mathrm{RCOOH} + \mathrm{NaOH} \longrightarrow -\mathrm{RCOO^-Na^+} + \mathrm{H_2O} \quad (1)$$

ester:

$$-\mathrm{RCOOR'} + \mathrm{NaOH} \longrightarrow -\mathrm{RCOO^-Na^+} + \mathrm{R'\text{-}OH} \quad (2)$$

* Corresponding author. E-mail: makmh73@yahoo.com.my

hydroxyl:

$$-ROH + NaOH \longrightarrow -RO^{-}\text{-}Na^{+} + H_2O \quad (3)$$

The main objective of this work was to determine the effects of physiochemical parameters (pH, dosage, stirring rate, concentration, contact time and temperature) on AB 25 adsorption onto base treated *Shorea dasyphylla* (BTSD). Understanding the mechanisms of AB 25 uptake is crucial, therefore, the characterization of the adsorbent by spectroscopy and quantitative analyses was performed.

1 Materials and methods

1.1 Reagents

AB 25 was purchased from Sigma Aldrich. The required concentration of solutions was prepared by diluting 1000 mg/L of stock solution of AB 25 with deionized water. The molecular weight of AB 25 is 416.4 g/mol and the molecular structure is given in Fig. 1. All other chemicals were of analytical reagent grade. The pH of AB 25 solution was adjusted by adding 0.1 mol/L HCl or NaOH solution.

1.2 Preparation of base treated *Shorea dasyphylla*

The dark reddish-brown colored sawdust of SD was collected from a wood processing industry in Penang, Malaysia and was sieved to a size of < 400 μm. One gram of SD was mixed with 50 mL (0.25 mol/L) NaOH solution and the mixture was stirred at 300 r/min for 1 hr at room temperature (300 K). The mixture was washed several times with deionized water to remove excess NaOH, and then dried overnight in an oven at 333 K. A dark effluent was noticed during washing the sawdust with deionized water, which according to Meena et al. (2008), would indicate the removal of lignin and base soluble extractives from the sawdust. The base treated *Shorea dasyphylla* was designated BTSD.

1.3 Characterization of BTSD

The pH of aqueous slurry (pH_{slurry}) was determined by adding 1.0 g of BTSD in 50 mL distilled water and stirred for 24 hr. It was then filtered and the final pH was measured. To determine the pH_{ZPC},1.0 g of BTSD was added in 50 mL (0.01 mol/L) KNO_3 solutions. The initial pH (pH_i) of solutions was adjusted from 2 to 10. After 24 hr of stirring, the final pH (pH_f) was recorded.

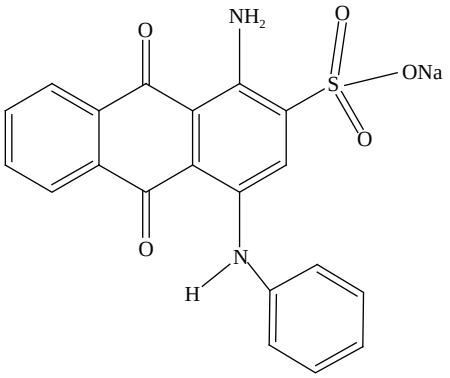

Fig. 1 Chemical structure of Acid Blue 25.

The value of pH_{ZPC} can be determined from the curve that cuts the pH_i axis of the plot ΔpH (pH_i–pH_f) versus pH_i. Sawdust is known to contain lignin, hemicellulose, cellulose and tannin as the major components (Gaballah et al., 1997; Gode et al., 2008). Various types of functional groups such as carboxyl, alcohols, amines, phenolic (Bulut and Tez, 2007), might be involved during the adsorption process. To identify the functional groups of SD and BTSD, Fourier transform infrared (FT-IR) (FT-IR System 1600 Model, PerkinElmer, USA) spectroscopy was carried out in the range of 400–4000 cm^{-1} using a KBr disc technique. The surface area and average pore diameter were determined using a Micromeritics ASAP 2010 gas adsorption surface analyzer according to the Brunauer, Emmett, and Teller (BET) multipoint technique. BTSD was degassed under vacuum for 24 hr at 343 K prior to BET analysis. The surface morphology of BTSD was analyzed using a scanning electron microscope (SEM, Leo Supra 50VP, Carl-Zeiss SMT, Germany).

1.4 Batch adsorption experiments

The effects of pH, adsorbent dosage, stirring rate, initial concentration and contact time on AB 25 adsorption were performed at room temperature (300 ± 1 K). BTSD with a weight of 0.1 g of was added into 50 mL (10 mg/L) solution of AB 25 and the mixture was stirred for 1 hr. The initial pH of AB 25 solution was fixed at 2 while the stirring rate was fixed at 500 r/min (unless otherwise stated). The effect of pH was studied at pH range of 2–6. The adsorbent dosage was studied by varying the weight of adsorbent from 0.01 to 0.10 g. The effect of stirring rate was studied by varying the stirring rate from 100 to 600 r/min. The kinetic study was carried out at three different concentrations of AB 25 (10, 20 and 30 mg/L). For isotherm study, the experiment was carried out at 300, 310 and 320 K using initial AB 25 concentrations of 10 to 70 mg/L. After adsorption, BTSD was filtered and the final concentration of AB 25 was recorded using UV-Visible spectrophotometer (U-2000 Model, Hitachi, Japan). The maximum wavelength (λ_{max}) of AB 25 value was 601 nm. Each adsorption experiment was conducted in duplicate and the average is taken as the results. The amount adsorbed and the percentage of AB 25 removed (R) was calculated using the following equations:

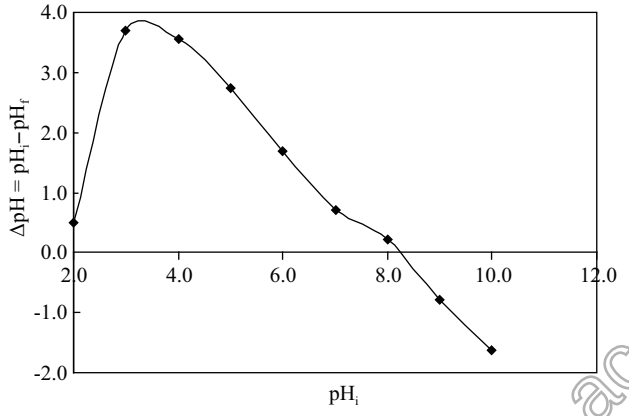

Fig. 2 pH_{ZPC} plot of BTSD.

$$q_e = \frac{C_0 - C_e}{W} V \tag{4}$$

$$R = \frac{C_0 - C_e}{C_0} \times 100\% \tag{5}$$

where, q_e (mg/g) is adsorbed or adsorption capacity, C_0 (mg/L) and C_e (mg/L) are the initial and final concentrations of AB 25, respectively; V (L) is the volume of AB 25 solution and W (g) is the weight of BTSD.

2 Results and discussion

2.1 BTSD characterization

It was found that BTSD is a basic adsorbent. The value of pH_{slurry} is 8.02. This is due to the presence of more nucleophilic groups such as $RCOO^-$ and RO^- on BTSD surface after the treatment with NaOH. The pH_{ZPC} is a characteristic that determines the pH at which the adsorbent surface has net electrical neutrality. In addition, it can give important information on electrostatic interactions between adsorbent and adsorbate. Anion adsorption is more favorable when pH is lower than the value of pH_{ZPC} since the surface of the adsorbent is positively charged (Ofomaja and Ho, 2008). The pH_{ZPC} plot for BTSD is shown in Fig. 2 and was determined as 8.25. Therefore, AB 25 will preferably be adsorbed at pH < 8.25. The SEM images at 500× magnification of SD and BTSD are shown in Fig. 3. The micrograph of SD particles (Fig. 3a) reveals low porosity and irregular surface structure. BTSD has a macroporous structure due to the presence of large pores (Fig. 3b). The BET and Langmuir surface areas of BTSD were 1.62 and 10.52 m^2/g, respectively. SD recorded BET and Langmuir surface areas of 1.59 and 10.44 m^2/g, respectively. Therefore, it can be concluded that base treatment did not cause a significant increase in surface area. The average pore diameter of BTSD, determined by Barrett-Joyner-Helenda (BJH) method, was 111.5 Å.

To confirm the presence of functional groups in the adsorbent, FT-IR analysis was conducted. Figure 4 presents the spectra of SD and BTSD before and after AB 25 adsorption. For SD, it can be seen that there is a broad and strong band from 2500 to 3600 cm^{-1}, which indicates the presence of carboxylic acid (RCOOH), alcohol (ROH) and amino (RNH_2) groups. This is consistent with the peaks at 1055 and 1163 cm^{-1} due to alcoholic C–O and C–N bending vibration (Wan Ngah and Hanafiah, 2008b). The band at 2907 cm^{-1} can be assigned to C–H stretching of the methylene group (Abdel-Ghani et al., 2007). SD spectrum also displays a strong band at 1730 cm^{-1}, which is assigned to the carbonyl group stretching from ester or the carboxylic acid group. The peak at 1616 cm^{-1} may be attributed to N–H bending or C=C stretching of the aromatic rings, while bands located at 1509 and 1461 cm^{-1} are the characteristic of amine deformation (Kamari and Wan Ngah, 2010). The peaks located at 1400–1600 cm^{-1} are assigned to aromatic skeletal vibrations. The strong peak observed at 1054 cm^{-1} might represent the C–O–C of an ether group. The band at 1245 cm^{-1} is assigned to phenolic hydroxyl group in lignin. The broad peak at 597 cm^{-1} is assigned to the bending modes of C–H group. After treatment with NaOH, the peak at 1730 cm^{-1} disappeared because base treatment resulted in the conversion of esters or carboxylic acid to carboxylate (Wan Ngah and Hanafiah, 2008b). The intensity of the peaks in the region of 1400 to 1600 cm^{-1} and at 1245 cm^{-1} for BTSD was reduced, possibly due to the removal of aromatic or lignin. However, after adsorption of AB 25, the peak at 1730 cm^{-1} appeared which indicated the presence of the carboxylic acid group since the AB 25 solution was acidic. The interaction between AB 25 and carboxylic, amino and hydroxyl groups was detected by the shift in wavenumber from 3415 to 3409 cm^{-1}. The peak at 1166 cm^{-1} that represented C–N bending vibration had shifted to 1159 cm^{-1} after AB 25 adsorption. All the findings from FT-IR spectra led to a conclusion that O and N-containing groups are the main adsorption sites for AB 25.

2.2 Effect of pH

The pH of the solution has a significant impact on the amount of AB 25 that can be adsorbed. pH can influence the dissociation of adsorption sites and the solution chem-

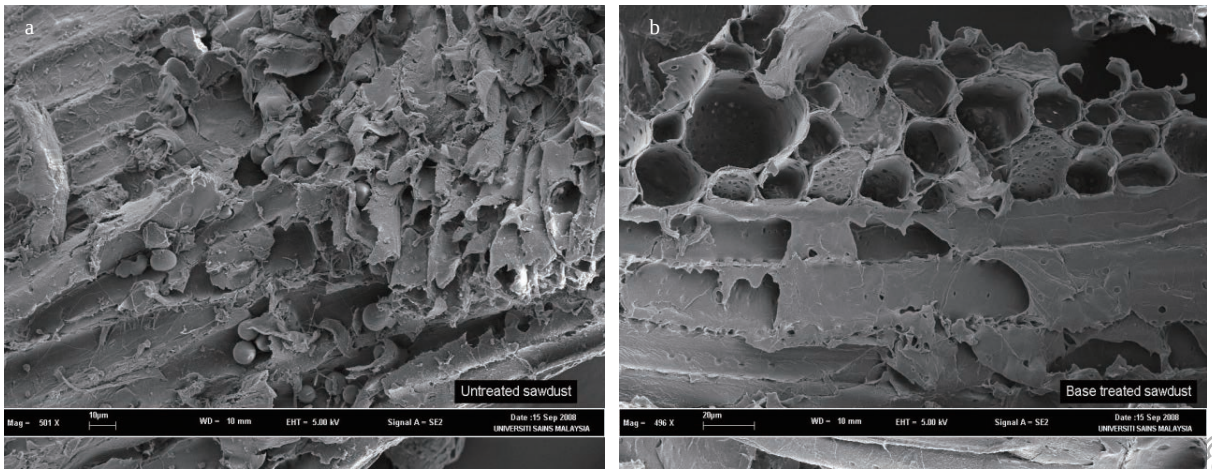

Fig. 3 SEM images of SD (a) and BTSD (b) at 500× magnification.

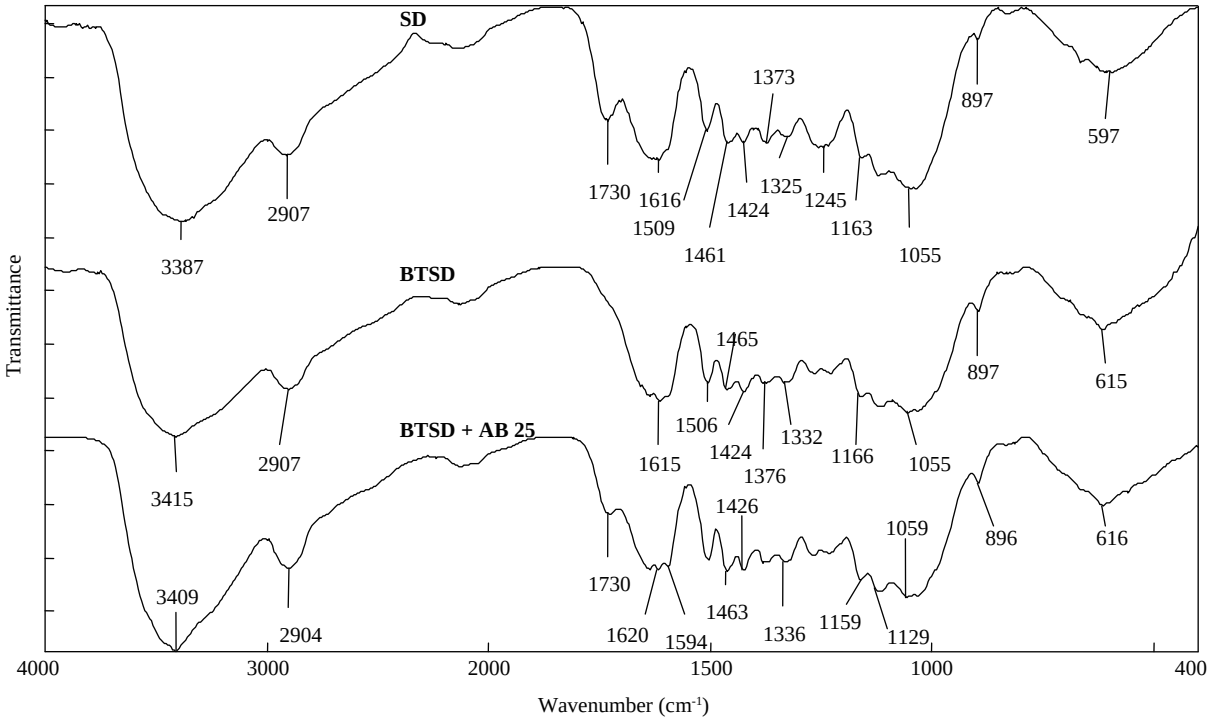

Fig. 4 FT-IR spectra of SD and BTSD, before and after AB 25 adsorption.

istry of AB 25, particularly the degree of ionization. The maximum amount of adsorption was observed at a very acidic condition (pH 2) but decreased with the increase in pH values (Fig. 5). A similar finding was reported by Tsang et al. (2007) in AB 25 adsorption by activated carbon. At a very low pH, the concentration of H^+ in the bulk solution would be high and the carboxyl, hydroxyl and amino groups of BTSD would be protonated, thus enhancing the electrostatic attraction between adsorbent and AB 25. In the aqueous solution, the sulfonate groups of AB 25 were dissociated and converted to anionic form as indicated below:

$$RSO_3Na \longrightarrow RSO_3^- + Na^+ \quad (6)$$

Therefore, the attraction between sulfonate groups and positively charged BTSD surface can be represented by Eqs. (7) to (9):

$$RCOOH_2^+ + RSO_3^- \Longleftrightarrow RCOOH_2^+ \cdots {}^-O_3SR \quad (7)$$

$$ROH_2^+ + RSO_3^- \Longleftrightarrow ROH_2^+ \cdots {}^-O_3SR \quad (8)$$

$$RNH_3^+ + RSO_3^- \Longleftrightarrow RNH_3^+ \cdots {}^-O_3SR \quad (9)$$

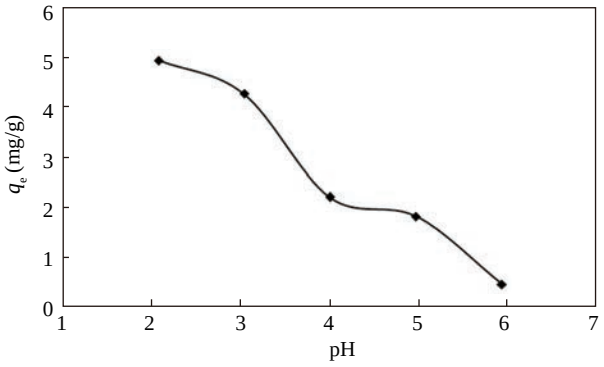

Fig. 5 Effect of pH on AB 25 adsorption.

As the pH increased, the number of positively charged adsorbent surface would be reduced. This would not favor the adsorption of AB 25 due to the reduction in the electrostatic attractions. In addition, due to the presence of various functional groups in BTSD as demonstrated by FT-IR spectra, other adsorption mechanisms such as hydrogen bonding and chemical adsorption could not be ruled out but require further investigation. Based on this finding, pH 2 was selected as the optimum pH for subsequent adsorption experiments.

2.3 Effect of dosage

The effect of BTSD dosage on the amount of AB 25 adsorbed was investigated for six different adsorbent dosages in the range 0.2–2.0 g/L and the results are shown in Fig. 6. It can be seen that adsorbent dosage is another important parameter that determines the amount of AB 25 adsorbed. As the dosage increased from 0.01 to 0.10 g, the percentage of AB 25 adsorbed also increased from 14% to 98%. At a low dosage, AB 25 molecules had to compete among each other due to low availability of BTSD surface area. Therefore, most of the dye molecules remained in the bulk liquid and the percentage of removal was very low. The highest amount of AB 25 adsorbed (q_e) at 0.01 g was attributed to the sufficient coverage of available adsorption sites on BTSD by AB 25. Due to low dosage, most of the adsorption sites on BTSD were covered by AB 25 molecules, which resulted in the highest amount of AB 25 adsorbed. However, a reverse trend was observed as the dosage was increased from 0.01 to 0.10 g. As the initial concentration of AB 25 in the solution was kept constant at 10 mg/L, an increase in dosage to 0.10 g would mean a surplus on the number of adsorption sites compared to AB 25 molecules. The accessible AB 25 molecules were insufficient to cover all the adsorption sites on BTSD,

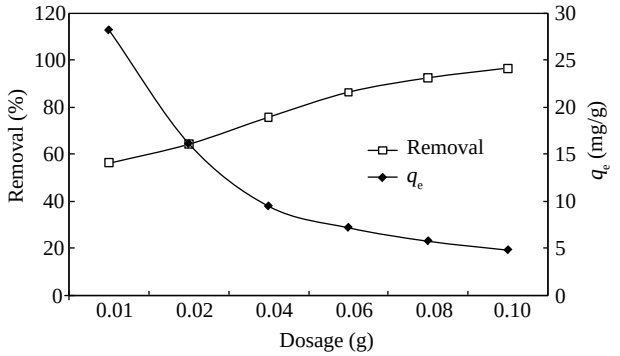

Fig. 6 Effect of BTSD dosage on AB 25 adsorption.

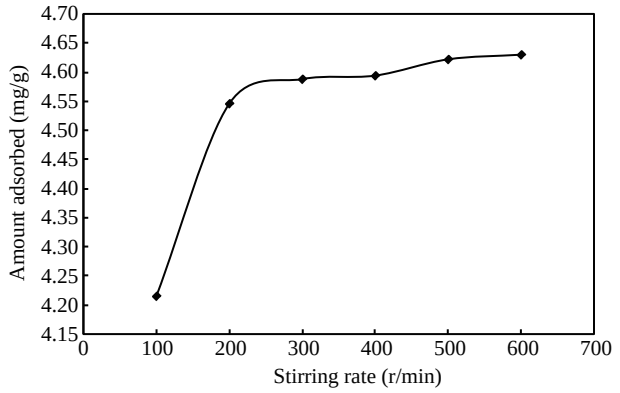

Fig. 7 Effect of stirring rate on AB 25 adsorption.

hence, resulting in the low amount of AB 25 adsorbed. Equation (4) also indicated an inverse relationship between q_e and adsorbent weight, therefore a decrease in the value of q_e was expected to be observed as more BTSD was added. Another important factor is attributed to a decrease in total surface area of BTSD and an increase in diffusion path length (Garg et al., 2004). The adsorbent dosage of 0.10 g was selected for subsequent adsorption experiments to ensure the maximum removal percentage of AB 25.

2.4 Effect of stirring rate

Stirring can influence the distribution of solute in the bulk solution and the formation of the external boundary film (Batzias and Sidiras, 2007). The study on the effect of stirring rate on AB 25 adsorption was carried out to find the optimum stirring rate. As shown in Fig. 7, at a higher stirring rate (> 200 r/min), there were more frequent collision between AB 25 and BTSD surface compared to lower stirring rate (100 r/min). According to Wan Ngah and Hanafiah (2008b), at a higher stirring rate, a good degree of mixing could be achieved, and the boundary layer thickness around the adsorbent particles could be reduced. Hence, the concentration of AB 25 near the BTSD surface would be increased. However, at stirring rate > 500 r/min, the amount of AB 25 adsorbed was found to remain constant. Thus, the stirring rate of 500 r/min was chosen as the optimum rate for the removal of AB 25.

2.5 Effect of concentration, contact time and kinetic of AB 25 adsorption

To establish an appropriate contact time, the amount of AB 25 adsorbed was measured as a function of time. Figure 8

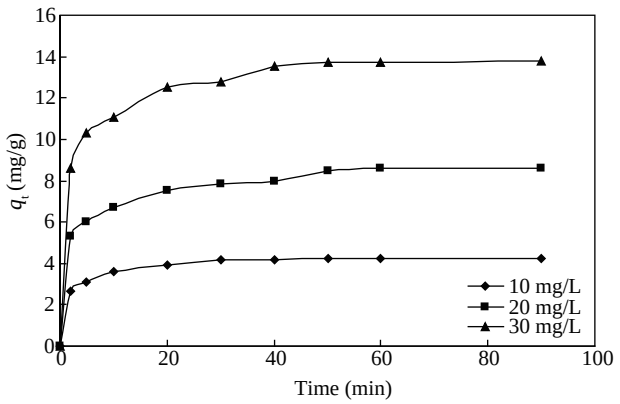

Fig. 8 Effect of concentration and contact time on AB 25 adsorption.

shows that as the initial concentration of AB 25 increased, the amount of AB 25 adsorbed was also increased. The equilibrium amount of adsorption increased from 4.25 to 13.77 mg/g with an increase in initial concentration from 10 to 30 mg/L. According to Kamari and Wan Ngah (2010), the increase in the amount of adsorption with increasing concentration was due to a higher probability of collision between adsorbate and adsorbent surface. Based on the graph, there was a rapid rate of AB 25 adsorption within 20 min and equilibrium was reached after 60 min. At the beginning of adsorption, the rate was fast because all the adsorption sites were vacant. However, as these sites were progressively covered, the rate of adsorption decreased.

To determine the adsorption kinetic of AB 25, the pseudo first-order (Ho and McKay, 1998) and pseudo second-order kinetic (Ho and McKay, 2000) models were applied as indicated by Eqs. (10) and (11), respectively:

$$\log(q_e - q_t) = \log q_e - \frac{k_1}{2.303}t \tag{10}$$

$$\frac{t}{q_t} = \frac{1}{k_2 q_e^2} - \frac{t}{q_e} \tag{11}$$

where, q_e (mg/g) and q_t (mg/g) are the amount of AB 25 adsorbed at equilibrium and at time t (min), respectively, k_1(1/min) is the pseudo first-order rate constant and k_2 (g/(mg·min)) is the pseudo second-order rate constant. The pseudo first-order model assumes that the rate of adsorption is proportional to the number of free adsorption sites. The straight-line plots of $\log(q_e–q_t)$ versus t were used to determine the rate constant (k_1), which can be obtained from the slope of the plots (plots not shown). According to Taty-Costodes et al. (2003), in most cases, the pseudo first-order equation did not apply well throughout the whole range of contact times and is generally applicable to the initial 20–30 min of the adsorption process. Although these plots show good linearity, the calculated values ($q_{e,calc}$) showed a large difference with the experimental values ($q_{e,exp}$). Therefore, the adsorption process did not follow the pseudo first-order model. The pseudo second-order kinetic model relies on the assumption that the rate-limiting step may be adsorption, involving valence forces through the sharing or exchanging of electrons between adsorbent and adsorbate (Ho and McKay, 1998). The straight line plots of t/q_t versus t were used to determine the amount

Table 1 Pseudo first-order and pseudo second-order constants at different concentrations of AB 25.

AB 25 conc. (mg/L)	$q_{e,exp}$(mg/g)	Pseudo first-order			Pseudo second-order		
		k_1 (1/min)	R^2	$q_{e,calc}$ (mg/g)	k_2 (g/(mg·min))	R^2	$q_{e,calc}$(mg/g)
10	4.24	0.09	0.990	1.67	0.14	1.000	4.35
20	8.57	0.08	0.905	4.84	0.04	0.999	8.84
30	13.74	0.07	0.987	5.41	0.03	1.000	14.12

of AB 25 adsorbed and the rate constant, which can be obtained from the slope and intercept (plots not shown), respectively. Based on the correlation coefficients (R^2) obtained, and comparison of the values between $q_{e,exp}$ and $q_{e,calc}$ (Table 1), the adsorption of AB 25 was best described by the pseudo second-order kinetic model since the values of R^2 were greater than 0.99 and the $q_{e,calc}$ values agreed with the experimental values ($q_{e,exp}$).

2.6 Adsorption isotherm

Adsorption isotherm is defined as the relationship between the amount of adsorbate adsorbed at a constant temperature and its concentration in the equilibrium solution. Isotherm is important for estimating the maximum amount of adsorbate adsorbed by a given amount of adsorbent. Figure 9 shows the adsorption isotherms at three different temperatures. According to classification of Giles et al. (1974), the isotherms seemed to be of the L-type, which indicated the monolayer coverage and AB 25 molecules were adsorbed in a flat wise manner on the surface of BTSD. Obvious difference between isotherms occurred at C_e > 10 mg/L. The adsorption process was further analyzed by two isotherm models, Langmuir and Freundlich. The Langmuir model is based on assumptions that adsorption occurs at specific homogeneous sites, energy of adsorption is constant and there is no transmigration of adsorbate in the plane of the surface, and is written as:

$$\frac{C_e}{q_e} = \frac{1}{Q_{max}b} + \frac{C_e}{Q_{max}} \tag{12}$$

where q_e (mg/g) is the amount of AB 25 adsorbed, C_e (mg/L) is the equilibrium concentration of remaining AB 25 in the solution, Q_{max} (mg/g) is the maximum amount of AB 25 adsorbed, and b (L/mg) is a constant that relates to the heat of adsorption. The value of maximum adsorption capacity was obtained from the slope of the plot of C_e/q_e versus C_e. The plots for the three different temperatures were found to be linear (plots not shown), and the maximum adsorption capacities of AB 25 by BTSD were 24.39, 22.32 and 21.01 mg/g at 300, 310 and 320 K, respectively (Table 2). These values were much higher than the value obtained by bamboo char (16.90 mg/g) as reported by Mui et al. (2010b). As fewer AB 25 molecules were adsorbed at higher temperatures, this was an indication of an exothermic adsorption process. The Freundlich isotherm model is derived to model the multilayer adsorption, applicable to a highly heterogeneous surface, and is given as:

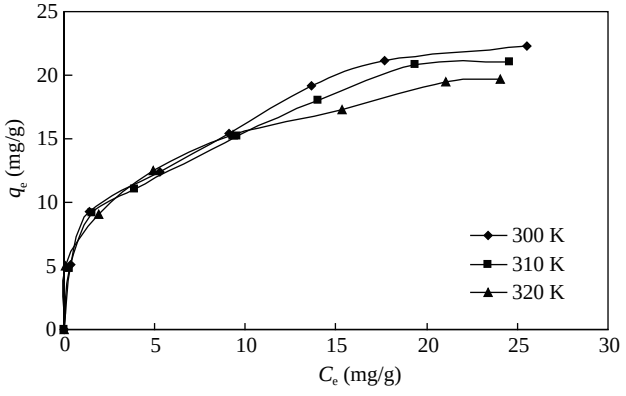

Fig. 9 Isotherm plots of AB 25 at different temperatures.

$$\log q_e = \log K_f - \frac{1}{n}\log C_e \tag{13}$$

where, K_f (mg/g) is maximum adsorption capacity and n is related to adsorption intensity. The plots were also linear (plots not shown) and the values of n were greater than 1 (Table 2), indicating that AB 25 molecules were favorably adsorbed by BTSD. Based on Table 2, Langmuir isotherm model was found to agree well with the experimental isotherm data.

2.7 Thermodynamic study

The Langmuir adsorption isotherm constants (b) obtained were used to calculate thermodynamic parameters such as Gibbs free energy (ΔG, kJ/mol), enthalpy (ΔH, kJ/mol) and entropy (ΔS, J/(K·mol)), as represented by Eqs. (14) and (15):

$$\Delta G = -RT\ln b \tag{14}$$

$$\ln b = \frac{\Delta S}{2.303R} - \frac{\Delta H}{2.303RT} \tag{15}$$

where, R is gas constant (8.314 J/(K·mol) and T(K) is the temperature.

The Van't Hoff plot of ln$b$ against 1/T (plot not shown) gave a straight line from which ΔH and ΔS were calculated from the slope and intercept, respectively. The observed thermodynamic values are given in Table 3. The negative values of ΔG at all temperatures indicated that the adsorption process was spontaneous and AB 25 has a good affinity for BTSD surface. However, as the temperature decreased, the ΔG values were found to have decreased, suggesting that AB 25 adsorption was less favorable at higher temperatures. The negative value of ΔH confirmed that the adsorption process was exothermic. The positive value of ΔS indicated an increase in randomness at the solid/solution interface after AB 25 adsorption on BTSD surface.

Table 2 Langmuir and Freundlich isotherm constants and correlation coefficients at different temperatures

Temperature (K)	Langmuir isotherm			Freundlich isotherm		
	Q_{max} (mg/g)	b (L/mg)	R^2	K_f (mg/g)	n	R^2
300	24.39	0.430	0.975	8.45	3.84	0.985
310	22.32	0.361	0.981	7.52	3.06	0.993
320	21.01	0.302	0.985	7.41	2.86	0.989

Table 3 Thermodynamic parameters of AB 25 adsorption

Temperature (K)	ΔG (kJ/mol)	ΔH (kJ/mol)	ΔS (J/(K·mol))
300	–32.19		
310	–30.72	–11.49	72.76
320	–29.28		

3 Conclusions

A new adsorbent produced from BTSD for AB 25 removal has been explored under batch mode. pH 2 was determined as the optimum pH for adsorption due to the strongest electrostatic attraction between positively charged BTSD surface and the negatively charged AB 25 molecules. The amount of AB 25 adsorbed was found to vary with dosage, initial concentration, contact time and temperature. A fast removal of AB 25 was noticed as more than 90% of AB 25 was removed in 60 min. The adsorption data fitted well to the Langmuir model and the recorded maximum adsorption capacity was 24.39 mg/g at 300 K. However, the adsorption capacity decreased with increasing temperature, an indication of an exothermic adsorption process. Adsorption kinetic was found to follow the pseudo second-order model. Due to the high availability and satisfactory rate of removal, BTSD can be a potential adsorbent for removing AB 25 from aqueous solutions.

Acknowledgments

The authors are indebted to the Universiti Sains Malaysia for the financial support (No. 304/PKIMIA/638056).

References

Abdel-Ghani N T, Hefny M, El-Chaghaby G A F, 2007. Removal of lead from aqueous solution using low cost abundantly available adsorbents. *International Journal of Environmental Science and Technology*, 4(1): 67–73.

Ali H, 2010. Biodegradation of synthetic dyes – A review. *Water, Air, and Soil Pollution*, 213(1-4): 251–273.

Anirudhan T S, Suchithra P S, 2009. Adsorption characteristics of humic acid-immobilized amine modified polyacrylamide/bentonite composite for cationic dyesin aqueous solutions. *Journal of Environmental Sciences*, 21(7): 884–891.

Atar N, Olgun A, 2007. Removal of Acid Blue 062 on aqueous solution using calcinated colemanite ore waste. *Journal of Hazardous Materials*, 146(1-2): 171–179.

Azlan K, Wan Saime W N, Lai Ken L, 2009. Chitosan and chemically modified chitosan beads for acid dyes sorption. *Journal of Environmental Sciences*, 21(3): 296–302.

Batzias F A, Sidiras D K, 2007. Dye adsorption by prehydrolysed beech sawdust in batch and fixed-bed systems. *Bioresource Technology*, 98(6): 1208–1217.

Bulut Y, Tez Z, 2007. Removal of heavy metals from aqueous solution by sawdust adsorption. *Journal of Environmental Sciences*, 19(2): 160–166.

Çolak F, Atar N, Olgun A, 2009. Biosorption of acidic dyes from aqueous solution by *Paenibacillus macerans*: Kinetic, thermodynamic and equilibrium studies. *Chemical Engineering Journal*, 150(1): 122–130.

Ferrero F, 2007. Dye removal by low cost adsorbents: Hazelnut shells in comparison with wood sawdust. *Journal of Hazardous Materials*, 142(1-2): 144–152.

Ferrero F, 2010. Adsorption of Methylene Blue on magnesium silicate: Kinetics, equilibria and comparison with other adsorbents. *Journal of Environmental Sciences*, 22(3): 467–473.

Gaballah I, Goy D, Allain E, Kilbertus G, Thauront J, 1997. Recovery of copper through decontamination of synthetic solutions using modified barks. *Metallurgical and Materials Transactions B*, 28(1): 13–23.

Garg V K, Amita M, Kumar R, Gupta R, 2004. Basic dye (Methylene Blue) removal from simulated wastewater by adsorption using Indian Rosewood sawdust: a timber industry waste. *Dyes and Pigments*, 63(3): 243–250.

Ghali A E, Baouab M H V, Roudesli M S, 2010. *Stipa tenacessima* L cationized fibers as adsorbent of anionic dyes. *Journal of Applied Polymer Science*, 116(6): 3148–3161.

Giles C H, Smith D, Huitson A, 1974. A general treatment and classification of the solute adsorption isotherm. I. Theoretical. *Journal of Colloid and Interface Science*, 47(3): 755–765.

Gode F, Atalay E D, Pehlivan E, 2008. Removal of Cr(VI) from aqueous solutions using modified red pine sawdust. *Journal of Hazardous Materials*, 152(3): 1201–1207.

Ho Y S, McKay G, 1998. A comparison of chemisorption kinetic models applied to pollutant removal on various sorbents. *Process Safety and Environmental Protection*, 76(4): 332–340.

Ho Y S, McKay G, 2000. The kinetics of sorption of divalent metal ions onto sphagnum moss peat. *Water Research*, 34(3): 735–742.

Kamari A, Wan Ngah W S, 2010. Adsorption of Cu(II) and Cr(VI) onto treated *Shorea dasyphylla* bark: Isotherm, kinetics, and thermodynamic studies. *Separation Science and Technology*, 45(4): 486– 496.

Liu Y, Zheng Y, Wang A Q, 2010. Enhanced adsorption of Methylene Blue from aqueous solution by chitosan-g-poly (acrylic acid)/vermiculite hydrogel composites. *Journal of Environmental Sciences*, 22(4): 486–493.

Meena A K, Kadirvelu K, Mishra G K, Rajagopal C, Nagar P N, 2008. Adsorptive removal of heavy metals from aqueous solution by treated sawdust (*Acacia arabica*). *Journal of Hazardous Materials*, 150(3): 604–611.

Mui E L K, Cheung W H, Valix M, McKay G, 2010a. Dye adsorption onto activated carbons from tyre rubber waste using surface coverage analysis. *Journal of Colloid and Interface Science*, 347(2): 290–300.

Mui E L K, Cheung W H, Valix M, McKay G, 2010b. Dye adsorption onto char from bamboo. *Journal of Hazardous Materials*, 177(1-3): 1001–1005.

Ofomaja A E, Ho Y S, 2008. Effect of temperatures and pH on methyl violet biosorption by Mansonia wood sawdust. *Bioresource Technology*, 99(13): 5411–5417.

Oladoja N A, Akinlabi A K, 2009. Congo Red biosorption on palm kernel seed coat. *Industrial & Engineering Chemistry Research*, 48(13): 6188-6196.

Özacar M, Şengil I A, 2005. Adsorption of metal complex dyes from aqueous solutions by pine sawdust. *Bioresource Technology*, 96(7): 791–795.

Saha P, 2010. Assessment on the removal of Methylene Blue dye using tamarind fruit shell as biosorbent. *Water, Air, & Soil Pollution*, 213(1-4): 287–299.

Shi X, Xiao B, Yang X, Zhou X, Li J, 2007. Batch study of dye removal from aqueous solutions by adsorption on NaOH-treated firry sawdust. *Fresenius Environmental Bulletin*, 16(12A): 1583–1587.

Taty-Costodes V C, Fauduet H, Porte C, Delacroix A, 2003. Removal of Cd(II) and Pb(II) ions, from aqueous solutions, by adsorption onto sawdust of *Pinus sylvestris*. *Journal of Hazardous Materials*, 105(1-3): 121–142.

Tsang D C W, Hu J, Liu M Y, Zhang W H, Lai K C K, Lo I M C, 2007. Activated carbon produced from waste wood pallets: Adsorption of three classes of dyes. *Water, Air, & Soil Pollution*, 184(1-4): 141–155.

Wan Ngah W S, Hanafiah M A K M, 2008a. Removal of heavy metal ions from wastewater by chemically modified plant wastes as adsorbents: A review. *Bioresource Technology*, 99(10): 3935–3948.

Wan Ngah W S, Hanafiah M A K M, 2008b. Biosorption of copper ions from dilute aqueous solutions on base treatedrubber (*Hevea brasiliensis*) leaves powder: kinetics, isotherm, and biosorption mechanisms. *Journal of Environmental Sciences*, 20(10): 1168–1176.

Wu J, Jung B G, Kim K S, Lee Y C, Sung N C, 2009. Isolation and characterization of *Pseudomonas otitidis* WL-13 and its capacity to decolorize triphenylmethane dyes. *Journal of Environmental Sciences*, 21(7): 960–964.